Title	Spectroscopic study of deep level emissions from acceptor defects in ZnO thin films with oxygen rich stoichiometry
Author(s)	Usman Ilyas, R. S. Rawat and T. L. Tan
Source	*COSMOS*, 9(1), 1-7
Published by	World Scientific Publishing Company

COSMOS, Vol. 9, No. 1 (2013) 1−7

DOI: 10.1142/S0219607713500043

World Scientific
www.worldscientific.com

SPECTROSCOPIC STUDY OF DEEP LEVEL EMISSIONS FROM ACCEPTOR DEFECTS IN ZnO THIN FILMS WITH OXYGEN RICH STOICHIOMETRY

USMAN ILYAS[*,†], R. S. RAWAT[*] and T. L. TAN[*]
[*]*NSSE, NIE, Nanyang Technological University*
1 Nanyang Walk, Singapore 637616
[†]*Department of Physics*
University of Engineering & Technology
Lahore, Pakistan 54890

Received 15 February 2013
Revised 25 March 2013
Accepted 11 June 2013
Published

This paper reports the tailoring of acceptor defects in oxygen rich ZnO thin films at different post-deposition annealing temperatures (500−800°C) and Mn doping concentrations. The XRD spectra exhibited the nanocrystalline nature of ZnO thin films along with inconsistent variation in lattice parameters suggesting the temperature-dependent activation of structural defects. Photoluminescence emission spectra revealed the temperature dependent variation in deep level emissions (DLE) with the presence of acceptors as dominating defects. The concentration of native defects was estimated to be increased with temperature while a reverse trend was observed for those with increasing doping concentration. A consistent decrease in DLE spectra, with increasing Mn content, revealed the quenching of structural defects in the optical band gap of ZnO favorable for good quality thin films with enhanced optical transparency.

Keywords: ZnO; structural defects and photoluminescence.

1. Introduction

Immense research work has been focused on making nonmagnetic semiconductors magnetic by doping them with small amounts (typically a few percentages) of magnetic atoms for spintronics applications. Such compounds are known as diluted magnetic semiconductors (DMS), because of the dilute concentrations of magnetic impurities. Of all diluted magnetic semiconductors and oxides, ZnO has provoked most interest and greater prospects in optoelectronic applications due to its direct wide band gap ($E_g \sim 3.37\,eV$).[1] The wide band gap of ZnO makes it transparent in the visible range which is maintained even at higher carrier concentrations, where ZnO shows metallic conductivity.[2] Moreover, the low threshold for optical pumping and large exciton binding energy (60 meV).[3,4] which is more than twice the thermal energy of GaN($k_BT = 25\,meV$),[5−7] allows lasing action in ZnO with extremely low pumping power at room temperature[8] and has been recognized as a promising photonic material in the UV region.[9]

However, one of the main obstacles in creating high quality ZnO-based optoelectronic devices is the unavailability of highly p-type ZnO thin films with significant hole carrier concentration. The main reason behind the difficulty in achieving p-type conductivity is the presence of native defects such as oxygen vacancies (V_o) and zinc interstitials (Zn_i) which are unintentionally introduced during the growth, making un-doped ZnO inherently an n-type material. In addition these structural defects also play an important role towards the ferromagnetic signal through Mn-defect pair ferromagnetic exchange coupling due to oxygen vacancies coupled with Mn ions.[10,11]

Photoluminescence (PL) spectroscopy, a contact less and nondestructive versatile technique, exhibits the electronic structure of the material by studying the possible electronic transitions between the defect states in the material. Light is directed onto a sample by a laser beam, where it is absorbed and imparts excess energy into the material in a process called photo-excitation. Photo-excitation causes electrons to move into permissible excited states within the material. When these electrons return to their equilibrium states, the excess energy is released and may include the emission of light (a radiative process) or may not (a nonradiative process). The most common radiative transition in semiconductors is between states in the conduction and valence bands, with the energy difference being known as the band gap energy. Radiative transitions in semiconductors also involve localized defect levels such as substitutional impurities (donors, acceptors) and native or intrinsic defects in ZnO crystals. The photoluminescence energy associated with these levels can be used to identify specific defects, and the amount of photoluminescence provides the quantitative information concerning the point defects such as vacancies, interstitials and impurities in the lattice. In general, radiative processes are associated with localized defect levels (intrinsic or substitutional), whose presence is detrimental to material quality and subsequent device performance.

It is of prime interest to study the activation and quantification of point defects in ZnO host matrix using room temperature photoluminescence and X-ray photoelectron spectroscopies (XPS) to get high quality thin films for optoelectronics. Moreover, the quenching of native defects, which are one of the sources that make the results controversial, is essential for the stability and reproducibility of the results concerned with the room temperature ferromagnetism (RTFM) in ZnO based thin films for their use in spintronic device applications.

2. Experimentation

2.1. *Preparation of nanocrystalline ZnO powder*

Nanocrystalline ZnO powder, used for preparing PLD pellets, with wurtzite structure was synthesized through a wet chemical method by a chemical reaction of 90 mMol zinc acetate dihydrate ($Zn(CH_3COO)_2 \cdot 2H_2O$) and 280 mMol potassium hydroxide (KOH) in an environment of 800 ml of methanol. The solution was continuously stirred magnetically (1100 rev/min) and heated at 52°C for 3 h. The solution was then allowed to cool and age at room temperature for 24 h. Precipitates formed after aging were removed from the solution by filtration. The precipitates, washed several times with distilled water, were centrifuged (2000 rev/min) to get rid of potassium completely from the solution. The precipitates were dried at 52°C in air to get solid powder.

2.2. *Thin film deposition using pulsed laser deposition (PLD)*

The powder obtained was palletized under a pressure of 10.5 metric tons and sintered at ∼1000°C for 12 h in air. The sintered pellet of ZnO was fixed on the target holder of the PLD system and was ablated by a second harmonic Nd:YAG laser (532 nm, 26 mJ) at pulse repetition rate of 10 Hz. The thin films were deposited on Si (100) substrate for constant ablation duration of 90 min in ultra-high vacuum of 10^{-6} Torr. Post-deposition annealing was carried out at different temperatures ranging from 500 to 800°C for 4 h in air and accordingly the thin film samples are referred as LD-0-500, LD-0-600, LD-0-700 and LD-0-800 in the text hereafter.

2.3. *Thin film deposition using spin coating*

Un-doped and Mn doped ZnO thin films with wurtzite structure were synthesized using spin coating technique. The Mn-doped ZnO thin films were prepared for four different Mn doping concentrations (0, 2, 5 and 10%) hereinafter referred as

SCD-0, SCD-2, SCD-5 and SCD-10 respectively. The thin films of these solutions were coated on Si (100) substrate at 3000 rev/min for 30 s using 6708D Desk-Top Precision Spin Coating System. After deposition with spin coater, the thin films were dried at 100°C for 5 min. The procedure from coating to drying was repeated 5−8 times to reach the desired thickness. The thin films were then annealed in air at 550°C for 2 h to improve their crystalline quality.

3. Results and Discussion

3.1. *XRD analysis*

The XRD spectral profiles of un-doped and Mn-doped ZnO thin films are shown in Fig. 1. The XRD profiles, showing polycrystalline hexagonal wurtzite structure, were matched well with space group $P6_3mc$ (No. 186) (ICSD # 82028) of wurtzite ZnO without any signature of impurity or binary zinc-manganese phase in the thin films samples.

The thin films grown by spin coating technique show a consistent decrease in crystalline quality with increasing Mn content in comparison to the un-doped one (SCD-0) as shown in Fig. 1. Moreover, the average crystallite size, calculated using the Scherer's formula, was estimated to be 17, 9, 7 and 6 nm for SCD-0, SCD-2, SCD-5 and SCD-10 respectively. The decrease in average crystallite size in turn reveals the deterioration in crystalline quality of ZnO. In addition, the strain induced due to the incorporation of Mn can also be cited as the possible reason of diffraction peak broadening resulting in a consistent decrease in crystallite size

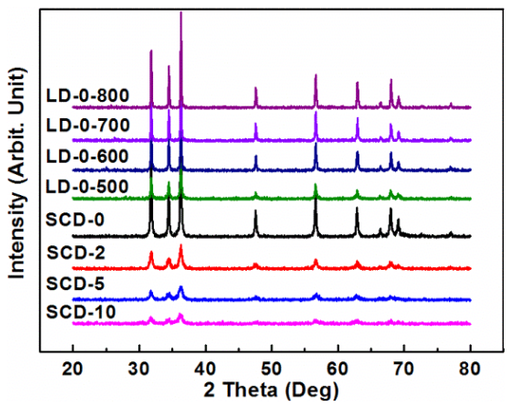

Fig. 1. XRD spectra of un-doped and Mn-doped ZnO thin films exhibiting polycrystalline nature.

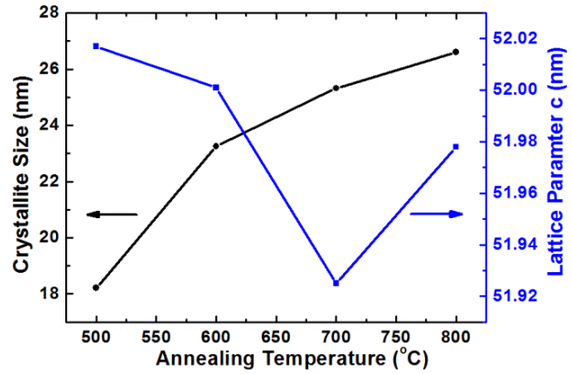

Fig. 2. Variation in crystallite size and lattice parameter '*c*', of ZnO thin films with the increase in the annealing temperature from 500 to 800°C.

with the increase in Mn doping concentration. A consistent increase in cell volume from 47.5 (for SCD-0) to 47.7 Å^3 was observed which reflects the incorporation of larger Mn^{2+}cations (0.83 Å) at the substitutional sites of Zn^{2+} (0.74 Å), without any degradation in the wurtzite crystal structure of host ZnO matrix.

However, the diffraction peak intensities, revealing the crystalline quality of ZnO thin films, were continuously improved with increasing post-deposition annealing temperature[12,13] of ZnO as is evident from Fig. 1. A consistent increase in crystallite size with increasing annealing temperature endorses the improved crystalline quality as is evident from Fig. 2. Moreover, the lattice parameter *c*, calculated using diffraction data of (002) peak, shows an inconsistent variation with increasing annealing temperature. This might be attributed to the variation in tensile/compressive stresses of ZnO coated silicon wafer due to the activation of certain point defects at different annealing temperatures. The minimum value of lattice parameter '*c*' at 700°C might be attributed to the reversion of zinc interstitials back to the lattice sites. The detailed analysis of temperature-dependent activation and variation of point defects will be discussed later using XPS and PL results.

3.2. *XPS analysis*

The compositional analysis of ZnO thin films (un-doped and doped ones) was performed by investigating the Zn 2p and O 1s core level XPS spectra after calibrating their binding energies by standard

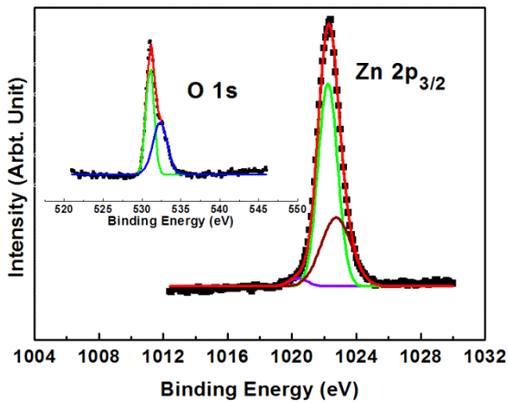

Fig. 3. Deconvoluted core level XPS spectra of Zn $2p_{3/2}$ and O 1s of the thin film annealed at 700°C.

C 1s peak (284.6 eV). The stoichiometry of all ZnO: Mn thin films calculated from the relative area under the curve of the zinc and oxygen peaks, after a Shirley background subtraction by nonlinear least square fitting, has been found to be oxygen rich with $Zn/O < 1$.

The main XPS spectra of LD-0-700 exhibiting core level binding energy peaks of Zn $2p_{3/2}$and O 1s are shown in Fig. 3. The Zn $2p_{3/2}$ spectrum exhibits slightly asymmetrical features indicating the possibility of existence of multi-component Zn. The asymmetrical Zn $2p_{3/2}$ with binding energies of 1021.5 and 1022.4 eV are observed which are related to elemental and oxide form of Zn, respectively.[14]

The Zn $2p_{3/2}$ peak of LD-0-700 was deconvoluted (using Gaussian peak fitting) into three peaks centered at 1020.4, 1022.2 and 1023.2 eV, respectively and is shown in Fig. 3.

The peak centered at 1022.2 eV represents the Zn^{2+} ions in stoichiometric ZnO[15] and represents the oxide form of Zn, while the peak at 1022.7 eV might be related to the native zinc vacancies which have been observed in the materials annealed at elevated temperatures.[16] The lower energy peak at 1020.4 eV is attributed to the zinc in oxygen deficient regions of ZnO host matrix.[15] It will reduce the charge transfer from zinc to oxygen thus increasing the shielding effect of the valence electrons in Zn ions which decreases the binding energy of the core electrons in the Zn ion. Thus, the deconvoluted XPS peaks at lower and higher energies in un-doped samples verify the presence of native zinc and oxygen vacancy defects which is also inferred through the PL analysis. Higher intensity of 1022.2 eV energy peak suggests that the majority of Zn atoms in the ZnO host matrix are in the Zn^{2+} state. Similar spectral features were observed for other samples annealed at different temperatures.

An inconsistent variation in Zn−O bonding (oxide form of Zn) was observed with Mn doping. The contribution of oxygen in Zn−O bonds was observed to be 47, 55, 80 and 49% for SCD-0, SCD-2, SCD-5 and SCD-10 respectively. Maximum value (80%) in SCD-5 reveals an enhanced concentration of oxygen in Zn−O bonding that in turn indicates minimum concentration of V_o in SCD-5.

The asymmetric O 1s XPS peak was deconvoluted with two peaks centered at ∼531.0 and 532.2 eV for the thin films annealed at 700°C (LD-0-700) as shown in Fig. 3. The deconvoluted peak centered at 531.0 eV is related to the O^{2-} ions in oxygen deficient regions within the ZnO matrix. The presence as well as the changes in the intensity of this component can be related to the variation in the concentration of oxygen vacancies.[17] Oxygen vacancies were found to be the dominant defects in thin films annealed at higher temperatures (700−800°C) which can result in reduction in lattice parameter '*c*' at higher temperatures. The higher binding energy peak (at 532.2 eV) is usually attributed to the chemisorbed or dissociated oxygen or hydroxyl (OH) species on the surface of the ZnO thin film[18] and related to oxygen interstitials.

The peak centered at ∼530 eV was also observed for thin films annealed at lower temperatures (500−600°C) which can be attributed to the O^{2-} ions on the wurtzite structure of the hexagonal Zn^{2+} ion array.[14,19] Based on these reports, the lower energy peak of oxygen spectrum is attributed to Zn−O bonds[20] which are dominant in the thin films annealed at lower temperatures. It can be inferred that higher temperatures (700 and 800°C) can cause oxygen vacancies to be produced in the thin film affecting the optical and electrical properties of ZnO.

3.2.1. *PL analysis*

The room temperature PL analysis was carried out to study the effect of Mn content and the annealing temperature on the concentration of structural defects and the band gap energy of ZnO thin films. PL spectra of un-doped and Mn doped ZnO thin films exhibit two emission bands in the UV and visible (mostly in yellow spectral region) regions, as shown in Fig. 4. The PL emission in UV region is the

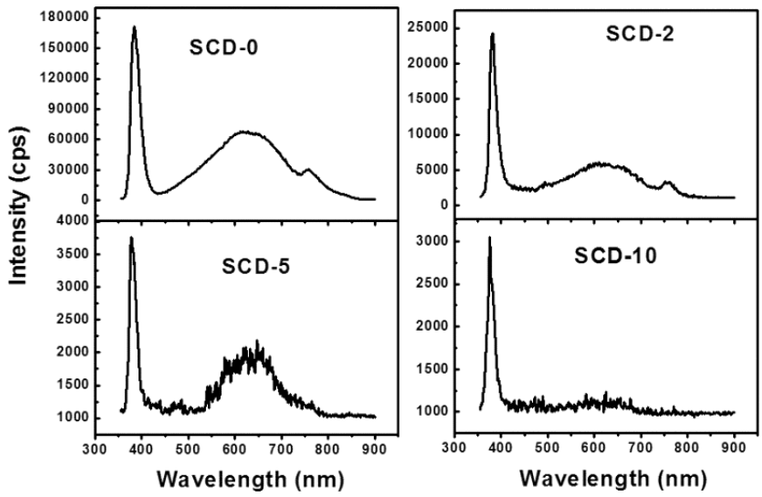

Fig. 4. PL emission spectra of un-doped and Mn doped ZnO thin films.

result of near band edge energy transitions from valence to conduction band while the deep level emissions in the visible region originates from structural defects such as Zn vacancy (V_{Zn}), oxygen vacancy (V_o), interstitial zinc (Zn_i) and interstitial oxygen (O_i).[21]

The UV band emission, centered at $\sim$380 nm, originals from the exciton recombination corresponding to the near band edge (NBE) exciton emission of the wide band gap ZnO.[22] The deep level emission (DLE) spectrum in green and yellow spectral regions,[23−25] which strongly manifests a polycrystalline structure[26] of ZnO, is due to a high density of native defects which exhibit different energies in DLE.[23]

The intensity of the UV emission peak (refer Fig. 4) strongly depends on the Mn content and decreases with increasing Mn content that might be attributed to some non-radiative recombination processes.[27] The UV emission peak shifts towards the shorter wavelength side (blue shift) from 383.6 to 375.9 nm (3.24−3.30 eV) with increasing Mn content from 0−10%, as is evident from Fig. 4. The blue shift can be the result of reduced average crystallite size of Mn doped ZnO thin films as estimated and discussed in Sec. 3.1.

From Fig. 4, it is evident that the deep level emissions (in the visible region) from the structural defects are significantly reduced with increasing Mn content as indicated by the marked decrease in the DLE peak intensity centered at about 624−633 nm. The relative contributions of different native (due to zinc and oxygen) and foreign (due to Mn) defects in DLE spectra can be evaluated by the estimation of relative intensities of the deconvoluted peaks. The deconvoluted DLE peak was found to be fitted, mainly, by two peaks centered at about $\sim$627 and 736 nm (not shown here). The peak at $\sim$736 nm is the second order reflection of the UV peak. The deconvoluted DLE spectral peak centered at $\sim$627 nm is attributed to the presence of O_i. Among all the doped thin films under investigation, SCD-5 was found to have maximum concentration of O_i (66.5%). The presence of O_i, due to oxygen rich stoichiometry in all thin film samples which is favorable to exhibit p-type conductivity due to the activation of acceptor states, as is reported in our previous study.[28] The activation of acceptor states also favors RTFM in Mn doped ZnO thin films.[29]

Moreover, it is inferred that the DLE spectral intensity is stronger in SCD-0 (un-doped sample) in comparison to doped ones, which in turn, reveals the quenching of native defects in doped samples (Fig. 4) and reduces the PL ratio (DLE/NBE). The reduced PL ratio in doped samples in comparison to un-doped ones reveals the improved optical transparency which is essential for transparent high power electronics and transparent conductive thin films.[2]

The temperature-dependent analysis of UV peak in PL emission has been carried out to study the effect of temperature on UV peak shift. The UV energy shifts towards the longer wavelength (red shift) from 3.24 eV to 3.0 eV with the increase in

temperature from 500 to 800°C that is in agreement to the results of Wang *et al.*[30] This red shift, which in turn reveals the reduction in optical band gap, can be attributed to the increased crystallite size as suggested by Van Dijke.[31] The increased crystallite size, due to grain growth at higher annealing temperatures, will result in a larger number of atoms in the particle causing greater splitting of energy levels and resulting in the shrinkage of the energy band gap. Moreover, the activation and concentration of native defects, with the increase in annealing temperature, can also be considered as a possible reason for the shrinkage of the energy band gap of ZnO.

Temperature dependent variation in native defects has also been studied for good quality ZnO thin films. Figure 5 shows the room temperature PL spectrum of ZnO thin films annealed at 600°C exhibiting two emission spectra in UV (at ∼382 nm) and deep level (mostly in the green and partly in the yellow spectral regions). The deconvolution of broad DLE peak, as seen in Fig. 5, shows its spectral features in green and yellow region with peaks centered at ∼481.4 nm (∼2.57 eV), 515.7 nm (∼2.40 eV), and 580.7 nm (∼2.13 eV). The peak related to 2.13 eV exhibits the signatures of yellow emission attributed to the O_i in ZnO thin films.[32] The evaluated energy of singly ionized Zn_i is 2.5 eV that is attributed to the transition from the energy level of singly ionized Zn_i to Zn vacancy (V_{Zn}) while 2.40 eV is related to oxygen vacancies (V_o) from the bottom of the conduction band to local defect energy level. The relative concentration of these native defects was estimated to be 31% (O_i), 34% (V_{Zn}) and 24% (V_o) in the un-doped sample (LD-0-600). The inset shows a consistent increase in DLE spectra with the increase in annealing temperature. Similar dominating native defects have been found in all the other samples annealed at different annealing temperatures. Singly ionized zinc vacancy (57%) in LD-0-500, oxygen interstitials in LD-0-700 (63%) and LD-0-800 (53%) were estimated to be the dominating native defects. These dominating defects are known to introduce acceptor levels in optical band gap which in turn is favorable for p-type conductivity in ZnO host matrix. Most of the calculations agree that O_i and V_{Zn} are favored under oxygen rich conditions, while Zn_i and V_o, are favored under Zn rich conditions.[33] Strong DLE spectra with maximum contribution from zinc vacancies and oxygen interstitials reveal that our thin film samples are indeed oxygen rich which is favorable stoichiometry for p-type conductivity in the ZnO host matrix.

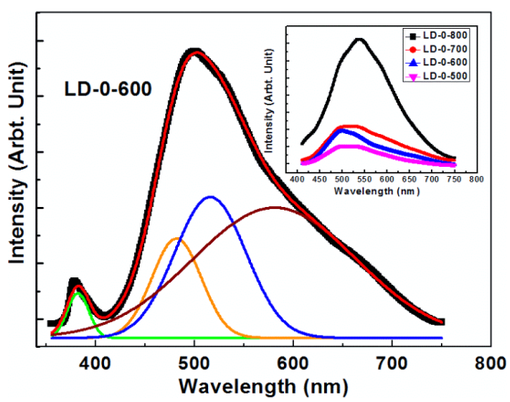

Fig. 5. Room temperature PL spectrum comprising near band edge and deep level emission bands of ZnO thin films. (Inset shows the variation in DLE spectra with temperature).

4. Conclusions

We have studied the tailoring of acceptor defects in oxygen rich ZnO thin films as a function of post-deposition annealing and Mn dopant concentration. The XRD spectra exhibited the nanocrystalline nature of ZnO thin films along with a consistent increase in cell volume with increasing Mn doping concentration. Temperature-dependent variation in lattice parameter '*c*' is estimated to be a minimum at annealing temperature of 700°C exhibiting the presence of oxygen vacancies. The detailed XPS analysis of Zn 2p and O 1s core level spectra revealed the presence of multi component zinc and oxygen in all the thin film samples complimenting the XRD results. NBE spectra revealed the red shift/blue shift in UV peak with increasing post-deposition annealing and Mn concentration, respectively. A consistent decrease in DLE spectra with increasing Mn concentration revealed the quenching of native defects in turn suggesting enhanced optical transparency. However, temperature-dependent DLE spectra revealed a consistent increase in the concentration of structural defects with maximum contribution coming from acceptor defects. The presence of dominant acceptor defects is favorable for p-type conductivity in the ZnO host matrix. To conclude, the optical and crystalline quality of un-doped and Mn doped ZnO thin films can be enhanced by tailoring the concentration of native defects.

References

1. Ohto Y, Hage T and Abe Y, *Jpn. J. Appl. Lett.* **36**: L1040, 1997.
2. Wang QP, Zhang DH, Xue ZY and Zhang XJ, *Opt. Mater.* **26**:23, 2004.
3. Look DC, *Mater. Sci. Eng.* **80**:381, 2001.
4. Reyonlds DC, Look DC, Jogai B, Liton CW, Gantwell G and Harsh WC, *Phys. Rev. B: Concdens. Matter* **60**:2340, 1999.
5. Özgür Ü, Alivov Ya I, Liu C, Teke A, Reshchikov MA, Dogan S, Avrutin V, Cho S-J and Morkoç H, *J. Appl. Phys.* **98**: 2005.
6. Fukumura T, Jin Z, Kawasaki M, Shono T, Hasegawa T, Koshihara S and Koinuma H, *Applied Physics Letters*, **78**:958, 2001.
7. Tiwari A, Jin C, Kvit A, Kumar D, Muth JF and Narayan J, *Solid State Commun.* **121**: 2002.
8. Ozgur U, Alivov Ya I, Liu C, Teke A, Reshcchikov MA, Dogan S, Avrutin V, Cho SJ and Morkoe H, *J. Appl. Phys.* **98**:41301, 2005.
9. Ko KJ, Chen YF, Yao T, Kobayashi I and Uchiki H, *Appl. Phys. Lett.* **76**:1905, 2000.
10. Chattopadhyay S, Neogi SK, Sarkar A, Mukadam MD and Yusuf SM, *J. Magn. Magn. Mater.* **323**:363, 2011.
11. El-Hilo M and Dakhel AA, *J. Magn. Magn. Mater.* **323**:2202, 2011.
12. Chen Y, Bagnall DM, Koh KTPHJ, Hiraga K, Zhu ZQ and Yao T, *Appl. Phys.* **85**:2595, 1999.
13. Kim KS, Kim HW and Kim NH, *Physica B* **334**:343, 2003.
14. Chen M, Wang X, Yu YH, Pie ZL, Bai XD, Sun C, Huang RF and Wen LS, *Applied Surface Science* **158**:134, 2000.
15. Taya YY, Lib S, Sun CQ and Chen P, *Appl. Phys. Lett.* **88**:173118, 2006.
16. Kelly A, Groves GW and Kidd P, *Crystallography and Crystal Defects*, revised edition (Wiley, New York, 2000).
17. Szorenyi T, Laude LD, Bertoti I, Kantor Z and Geretovszky Z, *J. Appl. Phys.* **78**:6211, 1995.
18. Major S, Kumar S, Bhatnagar M and Chopra KL, *Appl. Phys. Lett.* **49**:394, 1986.
19. Wang ZG, Zu XT, Zhu S and Wang LM, *Phys. E* **35**:199, 2006.
20. Li JH, Shen DZ, Zhang ZY, Zhao DX, Li BS, Lu YM, Liu YC and Fan XW, *J. Magn. Magn. Mater.* **302**:118, 2006.
21. Ilyas U, Rawat RS, Roshan G, Tan TL, Lee P, Springham SV, Zhang S, Fengji L, Chen R and Sun HD, *Appl. Surf. Sci.* **258**:890, 2011.
22. Yang LL, Zhao QX, Willander M, Yang JH and Ivanov I, *J. Appl. Phys.* **105**:53503, 2009.
23. Lin B, Fu Z and Yia Y, *Appl. Phys. Lett.* **79**:943, 2001.
24. Vanheusden K, Warren WL, Seager CH, Tallant DK, Voigt JA and Gnade BE, *J. Appl. Phys.* **79**: 1996.
25. Liu AHKM and Mascher P, *J. Luminesc* **54**: 1992.
26. Abrarov SM, Yuldashev SU, Kim TW, Kwon YH and Kang TW, *Optics Communications* **259**:378, 2006.
27. Zhang XT, Liu YC, Zhang JY, Lu YM, Shen DZ, Fan XW and Kong XG, *J. Cryst. Growth* **254**:80, 2003.
28. Ilyas U, Rawat RS, Roshan G, Tan TL, Lee P, Chen R, Sun HD, Fengji L and Zhang S, *J. Appl. Phys.* **110**:093522, 2011.
29. Dietl T, Ohno H, Matsukura F, Cibert J and Ferrand D, *Science* **287**:1019, 2000.
30. Wang YG, Lau SP, Lee HW, Yu SF and Tay BK, *J. Appl. Phys.* **94**:354, 2003.
31. Van Dijkin A, Meulenkamp EA, Vanmaekelbergh D and Meijerink A, *J. Lumin.* **90**: 2000.
32. Lukas Schmidt-Mende and Macmanus-Driscoll L, *J. Materials Today* **10**:40, 2007.
33. Janotti A and Valle CGVD, *Rep. Prog. Phys.* **72**:126501, 2009.